Dyes and Pigments 93 (2012) 1512–1518

Contents lists available at SciVerse ScienceDirect

Dyes and Pigments

journal homepage: www.elsevier.com/locate/dyepig

Dye/Clay intercalated nanopigments using commercially available non-ionic dye

Sumanta Raha*, Nurul Quazi, Ivan Ivanov, Sati Bhattacharya

School of Civil, Environmental and Chemical Engineering, RMIT University, 124 La Trobe Street, Melbourne VIC 3000, Australia

ARTICLE INFO

Article history:
Received 31 August 2011
Received in revised form
7 November 2011
Accepted 7 November 2011
Available online 15 November 2011

Keywords:
Nanopigment
Dye modification
Dye intercalation
Cationic dye
Clay
Azo dye

ABSTRACT

Two non-ionic azo dyes: solvent yellow 14 (SY14) and solvent red 24 (SR24), and one non-ionic disperse dye: dispersed red 60 (DR60) were chemically modified into their respective cationic species, which were then subsequently ion-exchanged with Na^+-montmorillonite in an acidic medium. The dye-intercalated montmorillonite was then centrifuged, dried and milled to prepare the pigment particles. X-ray diffraction studies on the pigments showed an increase in the basal spacing in the clay layers for the SY14 and DR60 based pigments NP14 and NP60 respectively, confirming intercalation of the dyes within the clay layers giving rise to a nano-structured system. The XRD pattern of the SR24 based pigment NP24 showed a diffused shoulder with a truncated peak, suggesting the possibility of a delaminated structure after adsorption of the dye. Due to the nano-structured morphologies, these pigments were classified as nanopigments. Thermogravimetric analysis showed different thermal stabilities for different nanopigments compared to the respective original dyes: an improvement in case of NP14, no change for NP24, and an apparent deterioration for NP60. The nanopigments were subsequently mixed with polypropylene to produce coloured specimens. Bleeding tests on these coloured specimens showed a reduction in leaching in turpentine.

1. Introduction

Both pigments and dyes are widely used as colourants for plastics. Dyes offer a wide range of colours, in combination with transparency, as they are dissolved in polymer [1]. This is however a cause of their disadvantage, as the mobility of dye molecules allows greater rate of migration and degradation, in comparison to pigments which are solid particles dispersed into the polymer matrix. Nevertheless, it is considered beneficial to replace some of the existing pigments (especially those based on heavy metals) with organic dyes or hybrid pigments based on dyes [2].

The idea of incorporating dyes into inorganic materials is not new [3]. Many commercial "Lake Pigments" were made by precipitating dyes with inorganic substrates [4]. If the inorganic substrate is a smectite clay or layered silicate, the most effective pathway was found to be using the ion-exchange process (Gemeay, 2002) [5]. For that reaction, the dye must exist in a cationic form, which is the case with basic or cationic dyes. Examples for that are intercalated products of Rhodamine dyes (Rhodamine B, Rhodamine 6G) with hectorite [6], montmorillonite [7–10], and other smectite clays [11–13]. Other basic dyes were also utilised, such as methylene Blue [14,15]. Majority of the research has focused on describing the influence of process parameters or dye structure on intercalate properties [16,17]. Attempts have also been made to commercialise the intercalates as nano-structured pigments by combining other organo-modifiers, such as quaternary ammonium salts with long alkyl chains [18].

In our laboratory, we have recently used cationic dye such as rhodamine for intercalation with clay to produce dye/clay hybrid nanopigments [10], by which we improved the thermal stability of the intercalated dye. UV exposure tests on coloured polypropylene/nanopigment composites showed a significant improvement in the photo-stability compared to the polypropylene/dye samples.

Unlike cationic dyes, which can be intercalated with clay, many other commercially available dyes are non-ionic. Examples of such non-ionic dyes include azo dyes and disperse dyes. Due to their non-ionic nature these dyes cannot be intercalated with clay by ion-exchange methods. To address this problem, chemical modification methods can be adopted using the chemical synthesis route to modify these commercially available dyes into their respective cationic species. Once modified into a cationic species, these dyes can then be intercalated or adsorbed on smectite clays to produce the dye/clay hybrid nanopigments.

In this paper, the authors report the synthesis of water soluble cationic dyes using two azo dyes, namely solvent yellow 14 (SY14) and solvent red 24 (SR24), and one disperse dye, disperse red 60

* Corresponding author.
E-mail address: sumanta_raha@yahoo.com (S. Raha).

0143-7208/$ – see front matter © 2011 Elsevier Ltd. All rights reserved.
doi:10.1016/j.dyepig.2011.11.003

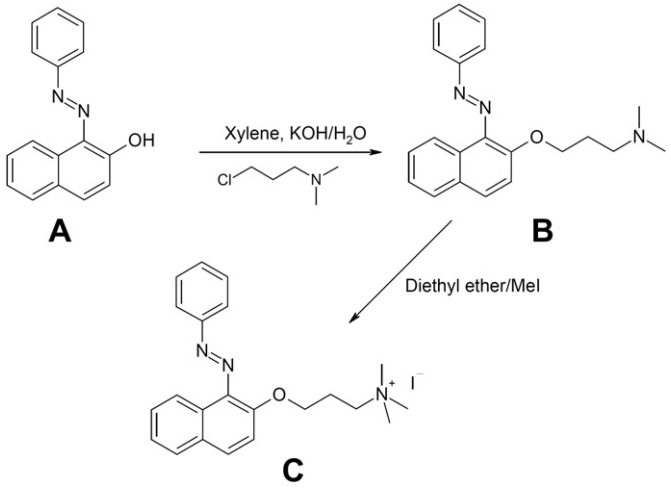

Scheme 1. Modification of the azo dye SY14.

(DR60), and their subsequent intercalation with Na+-MMT to form nano-structured pigments or nanopigments. This paper will also present X-ray diffraction (XRD) and thermogravimetric analysis (TGA) studies performed on these nanopigments.

2. Experimental

2.1. Materials

Dyes used in this work included two azo dyes, namely, Solvent Yellow 14 (SY14, CI 12055) and Solvent Red 24 (SR24, CI 26105), and one disperse dye, Disperse Red 60 (DR60, CI 60756), which were supplied by Allied Colors and Additives, Australia. Other chemicals used were: xylene (Merck), potassium hydroxide (BDH), 3-dimethylamino-1-propylchloride hydrochloride salt, and potassium carbonate (Aldrich). Na-montmorillonite used was Cloisite Na^+ from Southern Clay.

2.2. Molecular characterisation

Nuclear magnetic resonance spectra were recorded on a Bruker AM-300 spectrometer operating at 300.13 MHz (1H). The electrospray mass spectra were obtained on a Perkin–Elmer Sciex API-300 triple quadrupole mass spectrometer in positive ion mode with acetonitrile as solvent (uncertainty_0.3).

2.3. Chemical modification of dyes

The phenolic groups of the azo dyes SY14 and SR24 as well as Disperse dye DR60 can be alkylated using a suitable alkylating agent, such as 3-dimethylamino-1-propylchloride hydrochloride salt. Accordingly, these dyes were converted to their corresponding tertiary amines by reacting with 3-dimethylamino-1-propylchloride hydrochloride in the presence of potassium hydroxide in xylene under refluxing condition for 48 h. Usual work-up gave the corresponding amines. These amines were then treated with methyl-iodide in diethyl ether at room temperature, to give the desired salts as crystalline solids. The details of the reactions are given in the following Schemes 1, 2 and 3 respectively.

2.3.1. Synthesis of trimethyl-[3-(1-phenylazo-naphthalen-2-yloxy)-propyl]-ammonium iodide (C) (Scheme 1)

20 g of 1-Phenylazo-naphthalen-2-ol (SY14, A) were stirred with 300 ml of hot xylene. A solution of 5 g of potassium hydroxide in 20 ml of water was slowly added with stirring. The mixture was refluxed until the water was entirely removed. After cooling to about 70 C, the free base (prepared from 16 g 3-dimethylamino-1-propylchloride hydrochloride salt. with potassium carbonate and extraction with 50 ml of xylene) was added. The mixture was refluxed for 48 h, cooled to room temperature and filtered. The filtrate was distilled to dryness and the residue (B) was dissolved in 300 ml of ether and added 15 g iodomethane and stirred at RM for 48 h. The solid which separated was filtered off and washed with more ether to give the crude product. This was finally recrystallised from water to give the (20 g, 52%) pure product (C) as amino salt of SY14, mp.198–200 °C.

^{1}HNMR (DMSO-d_6): 2.16, m, 2H, CH_2; 3.00, s, 9H, $3CH_3$; 3.42, m, 2H, N–CH_2; 4.24, t, 2H, OCH_2; 7.46–8.25, m 11H, ArH. ESMS: $M^+ = 348.3$.

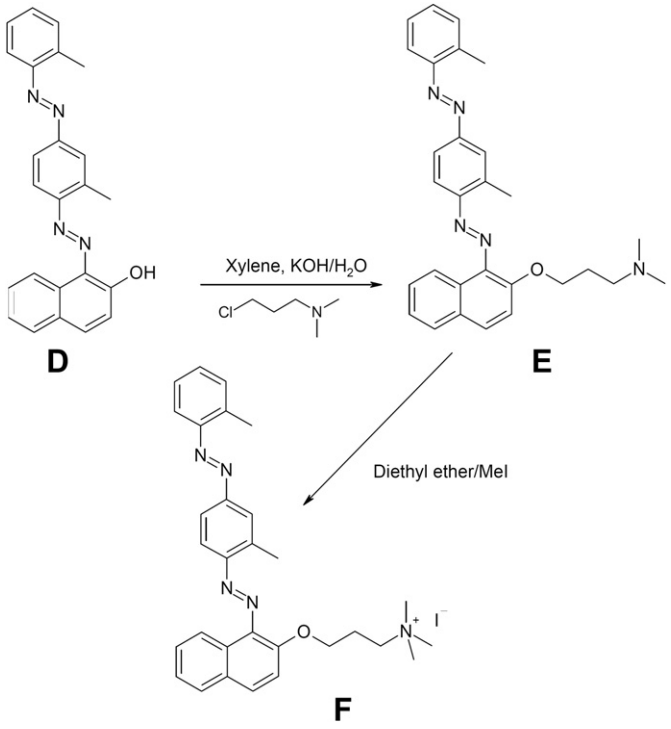

Scheme 2. Modification of the azo dye SR24.

2.3.2. Synthesis of trimethyl-{3-[1-(2-methyl-4-o-tolylazo-phenylazo)-naphthalen-2-yloxy]-propyl}-ammonium iodide (F) (Scheme 2)

20 g of 1-(2-Methyl-4-o-tolylazo-phenylazo)-naphthalen-2-ol (SR24, D) were stirred with 300 ml of hot xylene. A solution of 3.5 g of potassium hydroxide in 15 ml of water was slowly added with stirring. The mixture was refluxed until the water was entirely removed. After cooling to about 70 °C, the free base (prepared from 10 g 3-dimethylamino-1-propylchloride hydrochloride salt with potassium carbonate and extraction with 50 ml of xylene) was added. The mixture was refluxed for 48 h, cooled to room temperature and filtered. The filtrate was distilled to dryness and the residue (E) was dissolved in 300 ml of ether. 10 g Iodomethane was added and stirred at RM for 48 h. The solid which separated was filtered off washed with cold ether to give the crude product. This was finally extracted with diethyl ether using Soxlett extraction to give the (20 g, 62%) pure product (F) as amino salt of SR24, m.p. 88–90 °C.

^{1}HNMR (DMSO-d_6): 2.24, m, 2H, CH_2; 2.69, 3H, CH_3; 2.78, 3H, CH_3; 3.00, s, 9H, $3CH_3$; 3.46, m, 2H, N–CH_2; 4.32, t, 2H, OCH_2; 7.32–8.49, m 13H, ArH. ESMS: $M^+ = 480.3$.

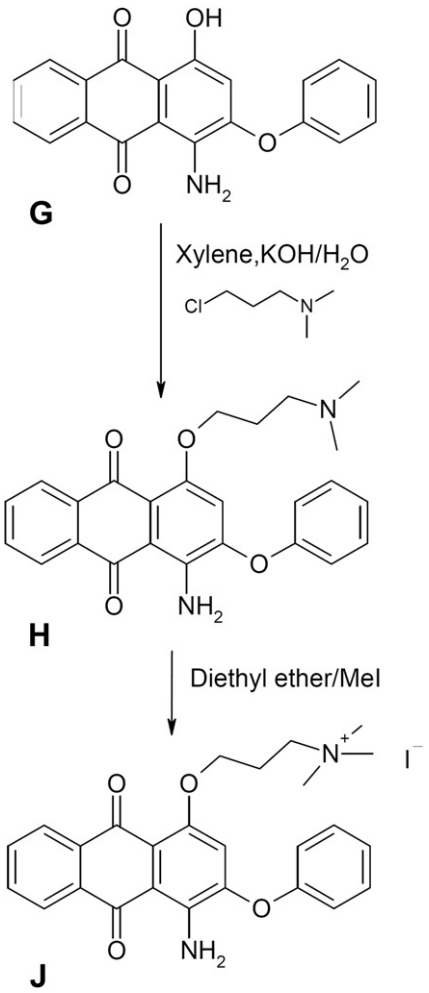

Scheme 3. Modification of the disperse dye DR60.

2.3.3. Synthesis of [3-(4-amino-9,10-dioxo-3-phenoxy-9,10-dihydro-anthracen-1-yloxy)-propyl]-trimethyl-ammonium iodide (J) (Scheme 3)

20 g of 1-Amino-4-hydroxy-2-phenoxy-anthraquinone (DR60, G) were stirred with 300 ml of hot xylene. A solution of 4 g of potassium hydroxide in 15 ml of water was slowly added with stirring. The mixture was refluxed until the water was entirely removed. After cooling to about 70 °C, the free base (prepared from 14 g 3-dimethylamino-1-propylchloride hydrochloride salt with potassium carbonate and extraction with 50 ml of xylene) was added. The mixture was refluxed for 48 h, cooled to room temperature and filtered. The filtrate was distilled to dryness and the residue (H) was dissolved in 300 ml of ether. 15 g iodomethane was added and stirred at RM for 48 h. The solid which separated was filtered off washed with more ether to give the crude product. This was finally extracted with water and separated the insoluble by filtration, removed the water soluble part under reduced pressure to give the (18 g, 55%) pure product (J), as amino salt of DR60, decomposition point: 248–250 °C.

^{1}HNMR (DMSO-d_6): 2.15, m, 2H, CH_2; 3.12, s, 9H, 3×CH_3; 3.57, m, 2H, CH_2; 3.96, t, 2H, CH_2; 6.81, s, 1H, ArH; 7.21, d, 1H, ArH; 7.29, t, 1H, ArH, 7.50, t, 2H, ArH, 7.85, m, 2H, ArH, 8.00, b, 2H, NH_2, 8.13, m, 1H, ArH, 8.02, m, 1H, ArH. ESMS: $M^+ = 431.50$.

Table 1
Nominal dye loadings in nanopigments.

Cationic Dye	Mol. wt.	Dye loading with 10 g Na+-MMT (100% CEC at 0.97 meq/g of clay)	Nominal dye loading in pigment
Modified SY14	475.37	4.6 g	31.5 wt%
Modified SR24	607.54	5.9 g	37 wt%
Modified DR60	558.42	5.4 g	35 wt%

2.4. Nanopigment preparation

The dye/clay nanopigments were prepared by ion-exchanging the cationically modified dyes with Na+-montmorillonite in an acidic environment. 10 g of Cloisite Na+ was dispersed in 300 mL of deionised water and was allowed to swell for 24 h. Separately, calculated amounts of the modified dyes were dissolved in 300 mL of HCl (1 M). An acid medium is generally found to be favourable for ion-exchanging of cationic dyes with clays (Arbeloa et al., 2005, Shamsipur and Azimi, 2001, Raha et al., 2009). The amount of the dyes was calculated from their respective molecular weights and the 100% cationic exchange capacity (CEC) of monmorillonite (0.97 meq/g). Each of the dye solutions was then slowly added to the swelled montmorillonite/water dispersion and stirred until a thick gel structure was formed due to the adsorption of the dye cations on to the negatively charged clay mineral layers (Lagaly, 2006). After mixing, the flocculated mixture was allowed to stand for another 48 h to allow sufficient time for the ion-exchange to occur. The mixture was left overnight, and then centrifuged at 4400 RPM for 20 min. The precipitated pigment was washed with sufficient amount of deionised water and dried at 80 °C for two days. The obtained cake was then crushed into smaller pieces, milled in a planetary ball-mill (Retsch PM100) and sieved through a 45 micron sieve to produce fine particles of the nanopigments. Table 1 presents the calculated amounts of dyes and the nominal dye loading for each of the three nanopigments produced.

2.5. X-ray diffraction characterisation

X-ray diffraction (XRD) studies on the clay and nanopigments were carried out using a Bruker AXS D8 wide angle X-ray diffractometer with Cu-Kα radiation ($\lambda = 0.154$ nm) at 40 kV acceleration voltage and 35 mA current. The basal spacing d_{001} was calculated from the 2θ peaks using the Bragg's law $n\lambda = 2d\sin\theta$.

2.6. Thermogravimetric analysis (TGA)

Thermogravimetric analysis (TGA) was carried out on the clay, dye and the prepared nanopigment to characterise their thermal behaviour. A Perkin–Elmer TGA-7 instrument was used and samples were heated from 50 °C to 700 °C at a rate of 20 °C/min under nitrogen at a purging flow rate of 20 ml/min. Beyond 700 °C the purging gas was switched to air and the samples were further calcined up to 800 °C.

2.7. Compounding with polypropylene

The polypropylene (PP) composites were prepared by mixing 1 wt% nanopigments in polypropylene (Basell Moplen HP301R) in an injection moulder at 190 °C. Maleated polypropylene (PP-MA) (Dupont Fusabond MZ109D) was also added at 5% as a compatibiliser for the clay/PP composites. For the reference, PP/Dye composites were also produced. The compositions of the PP composites are given in Table 2.

Table 2
PP composites and their compositions.

System	PP wt%	PP-MA wt%	Nanopigment wt%	Dye wt%
PP/NP14	94.00	5.00	1.00	–
PP/SY14	94.68	5.00	–	0.32
PP/NP60	94.00	5.00	1.00	–
PP/DR60	94.68	5.00	–	0.35
PP/NP24	94.00	5.00	1.00	–
PP/SR24	94.63	5.00	–	0.37

2.8. Colour measurements

A Minolta CR-300 colorimeter was used to measure the colour of the PP specimens in the CIE $L^*a^*b^*$ colour scale using 2° observer/D65 standard. The 2 mm thick specimens were placed on a white calibration plate (which had a measured $L^*a^*b^*$ colour value of 96.96, 0.08, 2.24). The colour difference ΔE^* was calculated using the CIE 1976 relation $\Delta E^* = \sqrt{(\Delta L^*)^2 + (\Delta a^*)^2 + (\Delta b^*)^2}$.

3. Results and discussion

3.1. Cationic dye synthesis

The key issue in this work was to make dye/clay intercalated nanopigments using commercially available non-ionic dyes. To intercalate a dye molecule in a clay particle, the dye needs to be ionic. Therefore, we have chosen two azo dyes, namely SY14 and SY24, (also known as Sudan I and IV respectively), as well as a disperse dye DR60 as the starting non-ionic dyes. The alkylation on the phenolic groups of SY14, SY24 and DR60 were little studied apart from methylation. At first, several reaction conditions [19] were attempted without any success. But then using a high boiling aprotic solvent, such as xylene using potassium hydroxide solution with 3-dimethylamino-1-propylchloride, we were finally able to get the intermediates and subsequent quarterisation gave the desired products in moderate yield.

3.2. XRD characterisation

Fig. 1 shows the XRD pattern of the cationically modified dye/clay nanopigments, as well as that of pure Na-MMT. The basal spacing of pure montmorillonite was found to be 1.16 nm. The modified SY14 based nanopigment NP14 showed a sharp and well-defined peak near $2\theta = 4.2°$, corresponding to a basal spacing d_{001} of 2.11 nm. It also showed another peak near $2\theta = 8.4°$, corresponding to the d_{002} planes (1.05 nm). The XRD pattern of NP14 clearly suggested a well-ordered stacked structure of the clay layers with an increase in basal spacing by 0.95 nm, thereby confirming the intercalation of the cationically modified SY14 with the clay layers.

The XRD pattern of the cationically modified SR24 dye based nanopigment NP24 showed a broad shoulder between 2θ close to 3.6° and 8.4°, and the disappearance of the original 1.16 nm peak of the pure clay. It suggests that NP24 was not exactly an intercalated system. The possible reason would be that due to the large molecular size and structure of this azo dye. Especially with two free-rotating azo links, it would be difficult to achieve an intercalated structure while maintaining a stacked packing of the clay layers. Instead, the XRD data suggests that due to the adsorption of the dye onto the clay surface, the clay layer was delaminated to form a nanopigment with a disordered house-of-card like structure.

The XRD pattern of the cationically modified disperse dye DR60 based nanopigment DR24 showed a weak shoulder at $2\theta = 4.2°$ (2.11 nm) and a peak near $2\theta = 6.6°$ (1.34 nm). It suggested that the dye was intercalated within the clay layer in two different orientations. It is possible that the majority of the intercalation occurred with a planar orientation of the aromatic rings, giving rise to a 1.34 nm basal spacing, whereas a fraction of the layers also had a non-planar orientation of the interacted dye resulting in a much large basal spacing of 2.11 nm.

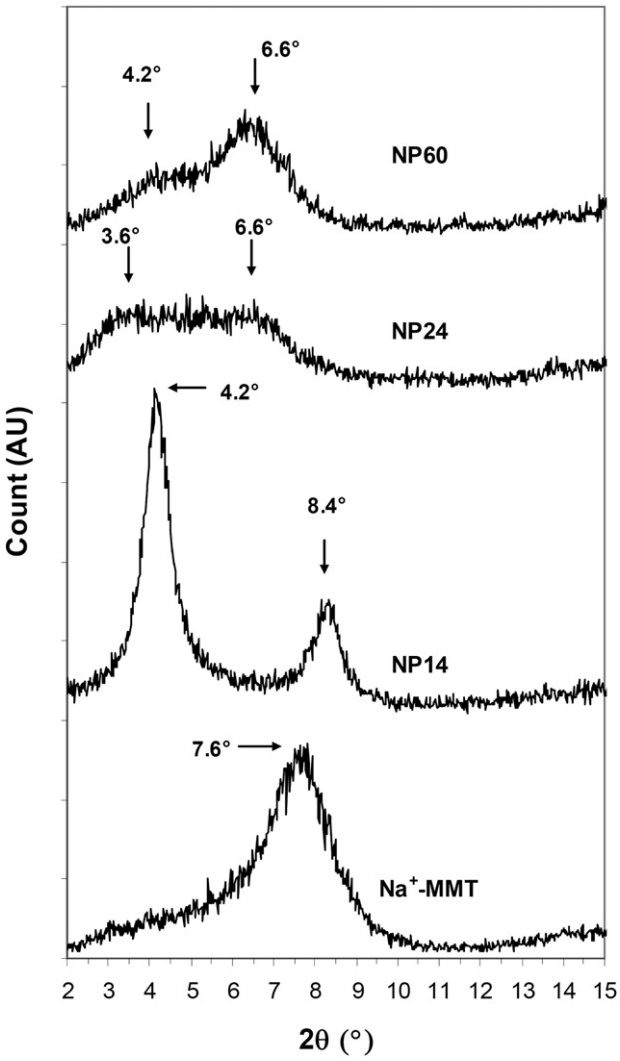

Fig. 1. XRD patterns of Na-MMT and the nanopigments.

3.3. Thermogravimetric analysis (TGA)

3.3.1. TGA results on the dyes

The TGA results on the dyes and the modified dyes given in Fig. 2, which presents the mass% as a function of temperature during heating under N_2 up to a temperature of 750 °C, and subsequent calcination in air up to 850 °C. The mass% data shows that, except for the dye DR60, there was almost no mass loss below 200 °C. The slight mass loss for DR60 in this range was possibly due to the presence of some bound moisture. Interestingly, the absence of an early moisture loss in the modified dyes indicated that in spite of being an iodide salt there were not moisture absorbing or hygroscopic. Above 250 °C all the dyes and modified dyes showed a sharp mass loss indicating the start of their thermal degradation. They also left some carbonaceous charred remains at the end of the heating stage under N_2, given by the difference in mass% between 700 °C and 850 °C, which can be attributed to the aromatic structure of these molecules.

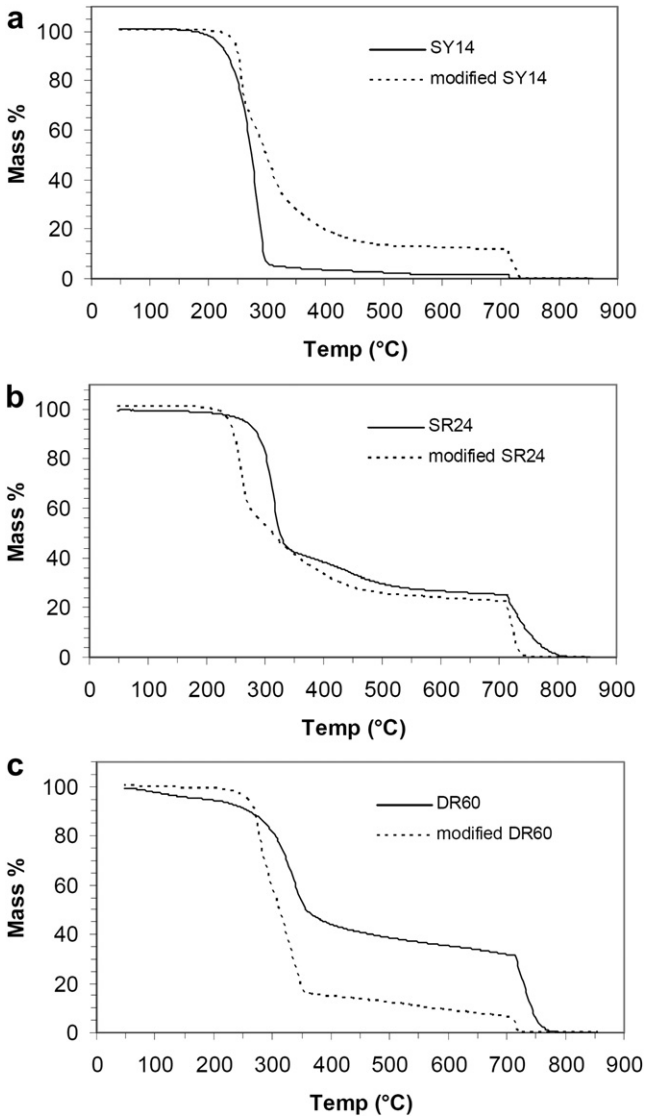

Fig. 2. TGA of dyes, cation-modified dyes and PP/compounds.

3.3.2. TGA results on the clay and nanopigments

Fig. 3 shows the TGA results performed on pure Na+-MMT and the nanopigments NP14, NP24 and NP60 during heating under N_2. The mass% data shows that pure clay had considerable amount of moisture content due to its hydrophilic nature, as indicate by the sharp drop in its mass below 100 °C. On the other hand, the three nanopigments NP14, NP24 and NP60 showed much lower moisture absorptions, suggesting a change from a hydrophilic to a hydrophobic nature due to the incorporation of the dye molecules. The two azo dye based nanopigments, NP14 and NP24, showed nearly identical mass loss percentage patterns from their TGA data, and they were also more stable compared with the disperse dye based nanopigment DR60.

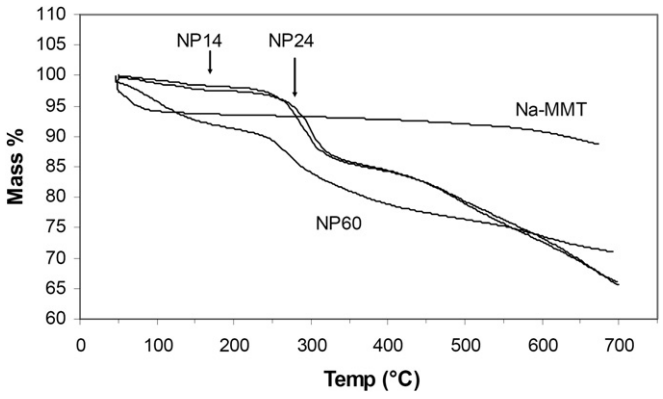

Fig. 3. TGA curves of pure clay and the nanopigments under N_2.

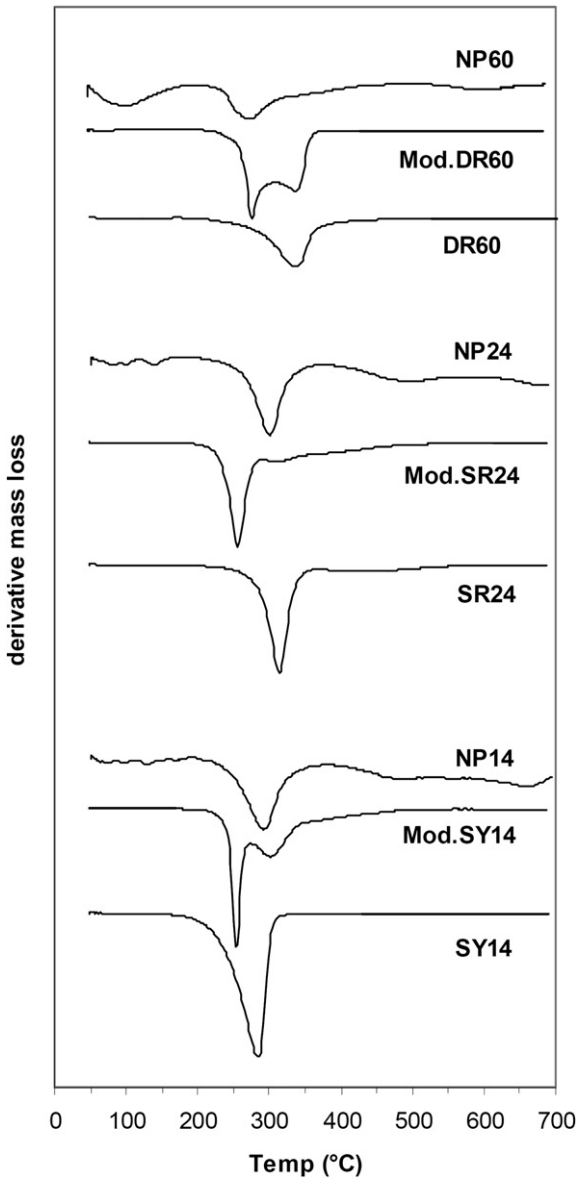

Fig. 4. Differential thermograms, under N_2. Vertical scales for NP14, NP24 and NP60 data have been magnified 5× for clarity.

3.3.3. Differential thermograms (DTG)

Fig. 4 presents the differential thermograms (DTG) of the dyes, modified dyes and the corresponding nanopigments, showing the derivative of their percentage mass loss as a function of temperature. The original dyes SY14, SR24 and DR60 showed peak decomposition temperatures at 286 °C, 316 °C and 338 °C respectively. Each of the modified dyes showed an early peak near 255 °C suggesting the release iodide anion and a possible conversion of the ammonium cation to a tertiary amine. The subsequent degradation

Table 3
Calculated dye loadings and estimated thermal stability of the nanopigments.

	Na^+-MMT	NP14	NP24	NP60
Mass at 180 °C (N_2)	93.61%	98.17%	97.52%	91.73%
Moisture content	6.39%	1.73%	2.48%	8.27%
Mass at 850 °C (air)	87.63%	60.98%	54.68%	55.36%
Mass at 850 °C (air, dry basis)	93.61%	62.12%	56.07%	60.35%
Calculated dye loading	–	32.4%	38.6%	29.7%
Estimated 10% dye loss temp in nanopigment	–	272 °C	288 °C	256 °C
10% mass loss temp. of original dye	–	232 °C	289 °C	285 °C

peaks for these modified dyes were observed at 303 °C, 312 °C and 337 °C, showing relatively similar peak degradation temperatures of the rest of the molecules of the modified dyes that contain the chromophores. In the nanopigment systems, particularly in NP14 and NP24, the absence of the iodine peak suggests successful ion-exchange and adsorption of the cationic dyes on the negatively charged clay layers. The DTG data for NP60, however, still showed the iodine peak, although reduced, in addition to the peak near 340 °C that appears like a shoulder due to the presence of the iodine peak. It suggests that the NP60 underwent a partial ion-exchange, with a fraction of the modified dye still remaining as salt and the other fraction adsorbed onto the clay layers by ion-exchange.

3.3.4. *Thermal stability of the nanopigments*

The thermal stability of the nanopigments was estimated at temperatures that relate to 10% mass loss, based on their dry mass at 200 °C. In the calculations, the dry mass loss of pure clay was also taken into account. The actual dye loadings in the nanopigments were calculated from the loss of dry mass after calcination at 850 °C.

It can be seen from Table 3 that dye loading calculated from TGA mass loss data matched very well with the nominal dye loadings (original weight of dye used) for the azo dye based nanopigments, indicating that almost all dye was adsorbed by the clay. However, for the disperse dye based nanopigment DR60, the calculated dye loading was found to be slightly less compared to the original loading, which suggests that some dye was lost due to incomplete adsorption. Table 3 also presents the estimated 10% mass loss temperatures of the dye in the nanopigment, which were calculated using mass balance and also considering the mass loss of clay itself. The values of the respective 10% mass loss temperatures of the original dyes are also given. As it can be seen, the azo dye SY14 based nanopigment showed an improvement of about 40 °C in the thermal stability of the dye after it was intercalated with the clay. The other azo dye SR24 based nanopigment NP24 showed almost equal thermal stability of the dye, showing no effect of its adsorption on the clay layers. On the other hand, for the disperse dye DR60 based nanopigment NP60, thermal stability was seen to decrease by about 29 °C. It was concluded that the apparent decrease actually reflects the loss resulting from a small fraction of iodide salt of the dye present in the pigment system as was evidenced by the DTG data in Fig. 4.

3.4. *Polypropylene/nanopigment coloured composites*

Fig. 5 shows the coloured specimens of the polypropylene composites prepared by melt-mixing PP with the nanopigments, and compares them with the coloured specimens prepared mixing the corresponding original dyes with PP. It can be seen that the clay based nanopigments incorporating the cationic species of the dyes gave similar colours compared with the original dyes. It was also found that there was a reduction in the brightness in the pigment

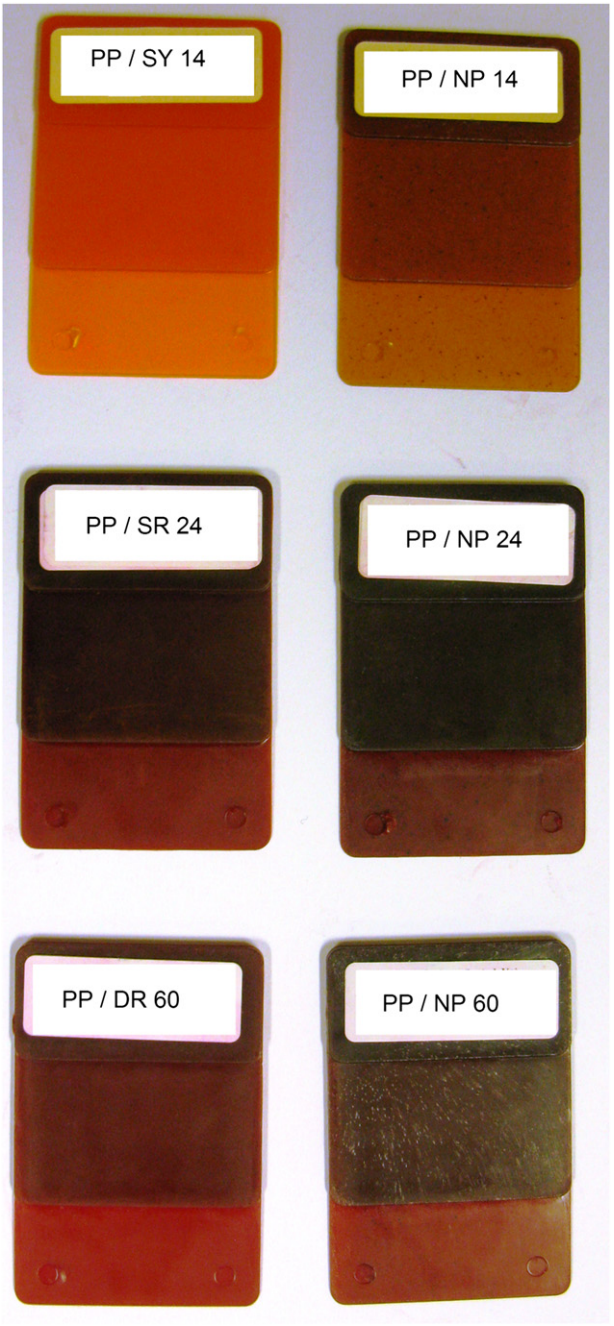

Fig. 5. Coloured polypropylene composites prepared by mixing the nanopigments and the corresponding original dyes.

samples, indicating some absorbance of the incident light due to the presence of the clay. Table 4 presents the colour values of the shown specimens and the corresponding colour difference between the dyed and pigmented samples.

3.5. *Bleeding tests*

Migration of dyes from polymers is an important issue. A common method to assess migration is by doing the bleeding test, where coloured specimens are shaken with solvents (e.g. turpentine) and colour of the solution is measured or assessed visually. In this test, 0.15 g of each composite specimen (Table 2) was placed in 15 ml of mineral turpentine. Table 5 gives a quantified measure of

Table 4
Measured colours of the PP composites and the colour change from dye to pigment.

Sample	$L^*a^*b^*$ colour scale	Colour difference ΔE^*
PP/SY 14	52.7, 37.4, 51.4	34.2
PP/NP14	38.0, 23.5, 23.8	
PP/SR24	27.9, 19.7, 6.2	10.2
PP/NP24	24.6, 10.7, 2.7	
PP/DR60	29.1, 25.6, 8.2	10.7
PP/NP60	27.3, 15.6, 4.8	

Table 5
Bleeding from coloured PP composites.

Composite	Absorbance (4 h)	Absorbance (24 h)
PP/SY14	0.236	0.592
PP/NP4	0.104	0.278
PP/SR24	0.155	0.397
PP/NP24	0.103	0.340
PP/DR60	0.028	0.168
PP/NP60	0.009	0.046

the bleeding by showing the absorbance of the migrated dye in solutions in 4 and 24 h. It can be seen that the bleeding from the nanopigment-based composites were less than original dye based composites, indicating that migration behaviour was improved after intercalation or adsorption of the dye within the clay.

4. Conclusions

Successful modifications of the non-ionic dyes SY14, SR24 and DR60 into their respective cationic species were confirmed by NMR study. XRD studies showed evidence of varying degree of dye intercalation or adsorption by the clay, indicating a nano-structured morphology of these nanopigments.

Thermal stability of these nanopigments was also found to vary from system to system. NP14 showed an improvement, NP24 showed the same stability, and NP60 showed a decrease in the thermal stability. It is thought that the intercalation of the modified SY14 dye within the clay layers was responsible for the improvement in its thermal stability. For the modified SR24 dye, the similar thermal behaviour was due to delamination of the clay layers with the dye adsorbed on the clay surface. Probably the lack of any protection that would be offered by the gallery space did not cause any improvement in its thermal behaviour. On the other hand, the apparent deterioration of the thermal stability for the nanopigment NP60 was attributed to the presence of a small fraction of iodide salt of the dye in the pigment system.

It was also observed that the use of the nanopigments in PP reduced the migration of the dye, which results from the intercalation/adsorption of the dye within the clay based pigments.

Acknowledgement

The authors thank Nanotechnology Victoria Ltd (NanoVic) for funding this research work. The authors also thank Allied Color and Additives Pty Ltd for supply of dyes and for providing access to their injection-moulding machine. The authors also acknowledge valuable comments from Prof. Shmuel Yariv of the Hebrew University of Jerusalem, Israel.

References

[1] Harris RM. Coloring technology for plastics. New York: William Andrew Publishing/Plastics Design Library; 1999.
[2] Bente LA. Dyes for the mass coloration of plastics. Plastics additives – an A–Z reference. London: Chapman & Hall; 1998.
[3] Giustetto R, Llabres i Xamena FX, Ricchiardi G, Bordiga S, Damin A, Gobetto R, et al. Maya blue: a computational and spectroscopic study. J Phys Chem B 2005;109:19360–8.
[4] Furmanski ER. FD&C Aluminium lakes HT food approved pigments for colouring plastics. Pacific Technical Conference and Technical Displays (Society of Plastics Engineers); 1979: 57–60.
[5] Gemeay AH. Adsorption characteristics and the kinetics of the cation exchange of Rhodamine-6G with Na+-Montmorillonite. J Colloid Interface Sci 2002;251:235–41.
[6] Windsor SA, Tinker MH. Electro-fluorescence polarization studies of the interaction of fluorescent dyes with clay minerals in suspensions. Colloids Surf A Physicochem Eng Asp 1999;148:61–73.
[7] Landau A, Zaban A, Lapides I, Yariv S. Montmorillonite treated with Rhodamine-6G mechanochemically and in aqueous suspensions: simultaneous DTA-TG study. J Therm Anal Calorim 2002;70:103–13.
[8] Pospisil M, Capkova P, Weissmannova H, Klika Z, Trchova M, Chmielova M, et al. Structure analysis of montmorillonite intercalated with rhodamine B: modeling and experiment. J Mol Model 2003;9:39–46.
[9] Klika Z, Weissmannova H, Capkova P, Pospisil M. The rhodamine B intercalation of montmorillonite. J. Colloid Interface Sci 2004;275:243–50.
[10] Raha S, Ivanov I, Quazi NH, Bhattacharya SN. Photo-stability of Rhodamine-B/montmorillonite nanopigments in polypropylene matrix. Appl Clay Sci 2009; 42:661–6.
[11] Lopez Arbeloa F, Tapia Estevez MJ, Lopez Arbbeloa T, Lopez Arbeloa I. Spectroscopic study of the adsorption of rhodamine 6G on clay minerals in aqueous suspensions. Clay Miner 1997;32:97–106.
[12] Lopez Arbeloa F, Lopez Arbeloa T, Lopez Arbeloa I. Characterization of clay surfaces in aqueous suspensions by electronic spectroscopies of adsorbed organic dyes. Trends Chem Phys 1996;4:191–213.
[13] Salleres S, Lopez Arbeloa F, Martinez V, Lopez Arbeloa T, Lopez Arbeloa I. Adsorption of fluorescent R6G dye into organophilic C12TMA laponite films. J Colloid Interface Sci 2008;321:212–9.
[14] Bujdak J, Iyi N, Fujita T. The aggregation of methylene blue in montmorillonite dispersions. Clay Miner 2002;37:121–33.
[15] Cione APP, Neumann MG, Gessner F. Time-dependent spectrophotometric study of the interaction of basic dyes with clays. III. Mixed dye aggregates on SWy-1 and laponite. J Colloid Interface Sci 1998;198: 106–12.
[16] Czimerova A, Bujdak J, Gaplovsky A. The aggregation of thionine and methylene blue dye in smectite dispersion. Colloids Surf A Physicochem Eng Asp 2004;243:89–96.
[17] Endo T, Shimada M. Optical properties of dyes incorporated into clay. Stud Surf Sci Catal 1991;60:189–96.
[18] Fischer H, Batenburg L. New nanopigments based on a combination of clay and organic dyes. Klei Glas Keramiek 2001;22:14–5.
[19] Crisp GT, Millan MJ. Conjugate addition of amino acid side chains to dyes containing alkynone, alkynoic ester and alkynoic amide linker arms. Tetrahedron 1998;54:649–66.